Michał KURPIŃSKI, Wojciech JAMROZIK
SILESIAN UNIVERSITY OF TECHNOLOGY, FACULTY OF MECHANICAL ENGINEERING
18a Konarskiego St., 44-100 Gliwice, Poland

Foreground extraction in images obtained in active thermography

Abstract

Detecting defects in adhesively bonded joints, using active thermography methods is very promising NDT testing method. In many cases, tests are made with agreed conditions, where a test object is always in specific place of IR camera view. Although, for needs of industry, system should be able to adjust Region of Interest in order to prevailing conditions. Therefore, it is necessary to develop appropriate method for this task. The paper describe one of the easiest attempt to separate foreground of an IR image sequence acquired by Lock-In Thermography (LT) and Pulse Thermography (PT). Proposed approach is based on segmentation and morphological operations. The IR image sequences of 11 various samples were used for this task. Obtained results show that elaborated technique of foreground object extraction is possible.

Keywords: active thermography, image processing, segmentation.

1. Introduction

Active thermography method is a very useful tool. In order, to obtain desirable results of subsurface defects, it is necessary to set a proper Region of Interest (ROI) as the beginning of overall processing procedure. In many cases, a ROI zone doesn't overlap with an IR camera's recording field. Therefore, in many cases, an suitable background subtraction method is required. The problem is frequent in an industrial environment. It is hard to adjust a test object in the specific position each time. This issue becomes important, when several objects from different IR images have to be compared between each other. In many cases, classic foreground detection methods couldn't be applied to infrared images. Mostly, they use time information to separate moving objects from a static background. Unfortunately, it is unhelpful in situations, where background and the object are static. Besides, the temperature variation between background and observed sample's surface is mostly too low. In some cases, the specimens could be recognized by simple methods like image segmentation algorithms (region growing, region splitting, etc.) [1]. More often, to make the separation procedure possible, an appropriate processing method is required. There are many possible approaches, suitable for regular IR image processing algorithms [2]. Those methods are well specialized in rising contrast between defects present in the sample e.g. contaminations, layer detach, etc., but often cannot be directly used for background separation purposes. The noise of an IR camera and environment also generates additional issues. The paper shows steps of the foreground extraction procedure. Firstly, the best processing methods are used to highlight differences between specimen and the background. Next, automated foreground ROI extraction algorithm cuts an appropriate sector of an image. Presented approach is a part of a complex NDE system for adhesive joints.

2. Materials

As the result of Authors' recently performed research, many various data sets were gathered. Stored data are sequences of IR images recorded during active thermography tests, where various test conditions were verified. Tested specimens were 150×75 mm steel sheets bonded by specific path of adhesive to create a sandwich structure. Shape of the adhesive path and other additional factors are desired to test active thermography methods effectiveness and noise resistance (Tab. 1). There were 11 different kinds of samples in total.

Tab. 1. Schemes of all samples used in tests

Symbol	Description	Scheme
GR	Three separated sectors of adhesive with different thickness	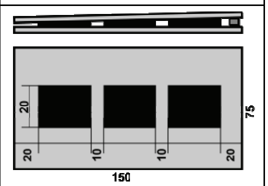
DIS5 DIS10 DIS15	One regular path of adhesive with gap: 5, 10 or 15 mm	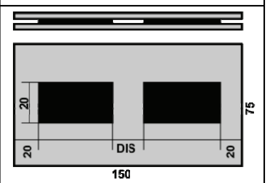
OIL1 OIL2	One regular path with oil drops of surface	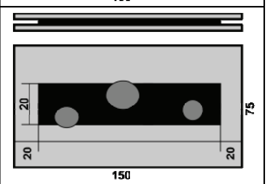
WV	One regular path with waved steel sheet from one side	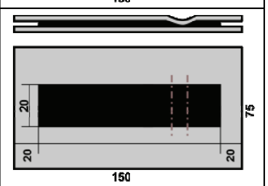
SZC	Two thin paths of adhesive along the sample with unregular gap between them	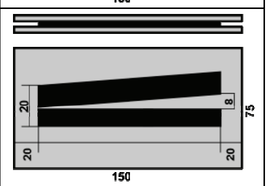
POG	Sample contains three steel sheets, and two layers of adhesive sector with paths with different length of gap	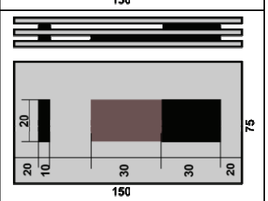
VAR	Ten squares of adhesive with side from 20 to 2 mm of length	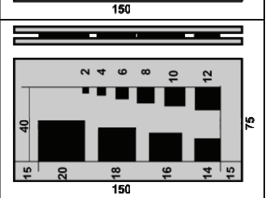
TRI	Path of glue with triangle-like shape	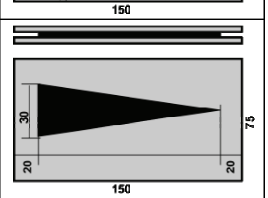

As an earlier research shown, it is possible to obtain valuable results for the presented test specimens by the given acquisition parameters. Therefore, the test sequences were obtained by Lock-In Thermography (LT) and Pulse Thermography (PT) methods [3]. Two sets of data were acquired by PT testing procedure with 550 ms and 750 ms of thermal excitation with approx. 6 s delay.

The third set was obtained by LT testing procedure with harmonically modulated excitation heat stimulation in frequency of 0.016 Hz. In summary, the data base has 66 sequences of IR images (3 methods and two sides of 11 samples). Besides, in consecutive test procedures, the position of samples and IR camera changes repeatedly. An large timespan between consecutive tests, the test chamber simplicity and possible operator's errors are the most possible factors. It would be easy to extract observed object in visible range because of samples' black painting. Actually, some industrial IR cameras are able to integrate IR view with visible light edges contour [5]. This technique uses view of second regular visible light camera, embedded into the device. Data acquired by Authors contain only IR images, therefore an appropriate software solution has to be developed.

An heating characteristic makes differences which may affect the processing method choice. Temperature value of IR image pixels of LT sequences change periodically, while in PT methods they have sharply visible step of heating and cooling period (Fig. 1). Therefore, single, universal method can be ineffective.

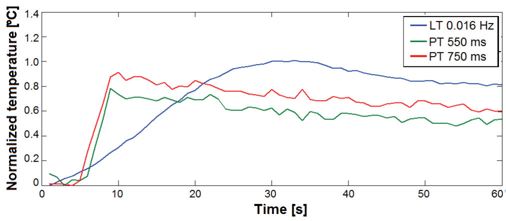

Fig. 1. Temperature measurement changes of chosen pixel during different test methods and parameters in relation to minimal temperature in every sequence (LT 0.016 Hz – Lock-In method with 0.016 Hz frequency of harmonic thermal stimulation; PT 550 and 750 ms – Pulse Thermography with 550 and 750 ms of step heat sequence duration accordingly)

To show the problem of temperature irregularity on corresponding IR images, some of chosen VAR sample (Tab. 1) images are put into Tab. 2.

3. Chosen contrast increase methods

A raw sequence of IR images of any active thermography acquisition method needs additional preprocessing operation before a proper thresholding method could be applied. It is necessary to perform data reduction and improve background-object ratio. The first step is to increase contrast between background and sample surface as much as possible. There are many processing methods that can be used for this task [2]. Nevertheless, many of them are too complex and suitable only for further, certain data processing algorithm. The most required feature is a good background separation in every direction. To simplify ROI automated selection, several available methods were implemented and evaluated:

- Fast Fourier Transform (FFT) –Phase and Amplitude Image [3]
- Principal Component Thermography (PCA) [7]
- Histogram Operations (cutting highest and lowest group of pixels, which number of bins are below 10% of the highest number of bins) [5-7],
- Correlated Contrast [7].

Image processing methods were implemented as a Matlab function and used to process a part of data base. Unfortunately, histogram was not appropriate for selected data. Mostly, background and sample surface pixels values stays heterogeneous after processing, so output images cannot be used in further thresholding procedure. Other methods are more promising. For LT IR images FFT phase image presents the best possible contrast between sectors. For PT method, IR images both – Correlated Contrast and Amplitude image are satisfying. Moreover, Correlated Contrast method provides better uniformity and homogeneity of background at the PT images. Exemplary results for the VAR sample (Tab. 1) are presented in Tab. 3.

Tab. 2. Chosen IR images of data use in tests (raw data)

No.	PT 550 ms	PT 750 ms	LT 0.016 Hz
DIS15 Front Side	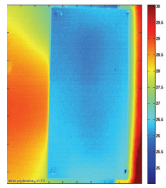	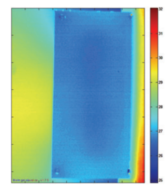	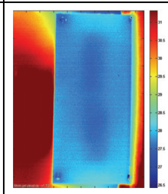
TRI Front Side	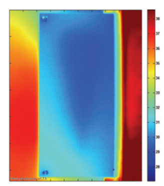	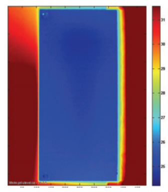	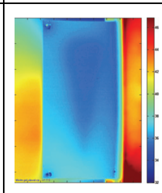
VAR Front Side	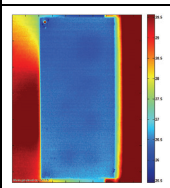	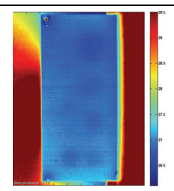	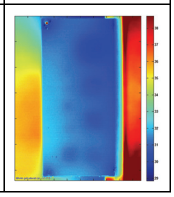

Tab. 3. Chosen IR images of data with different processing methods

No.	PT 550 ms	PT 750 ms	LT 0.016 Hz
Histogram	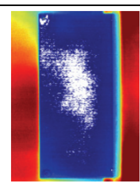	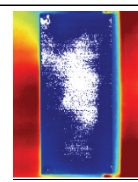	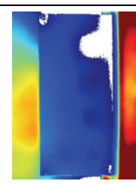
Correlated Contrast	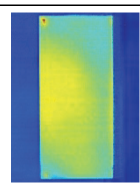	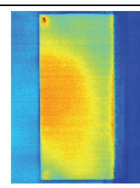	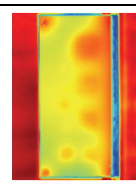
FFT Amplitude	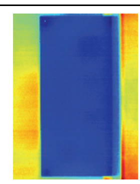	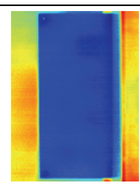	
FFT Phase	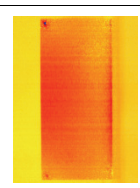	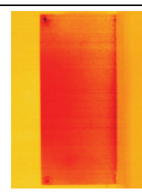	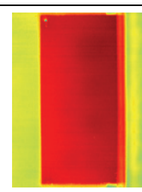
Principal Component Thermography			

It is necessary to ensure visual considerations by appropriate assessment solution. All images (Tab. 3) were cut horizontally and vertically through a point in the image center. Then, acquired profiles were manually divided into the values of specimen and background sectors. This procedure is visualized in Fig. 2.

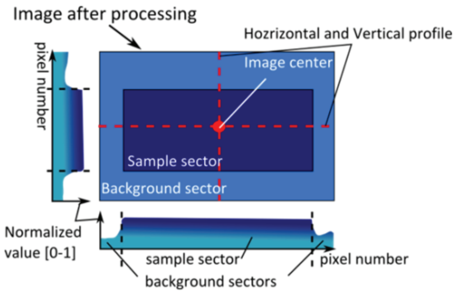

Fig. 2. Setting a sample and background sectors of vertical and horizontal profiles of a various methods images

In the next step, the sectors of profiles (background and sample) are used to compute differences in contrast between them. Firstly, all scales of the images were normalized to [0,1] range, so values of the profiles could be compared between various methods. Chosen profile of all the methods are presented in Fig. 3.

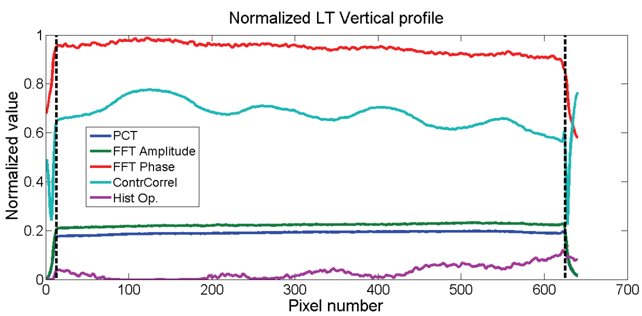

Fig. 3. Example profile of a *VAR* sample tested using LT method with 0.016 Hz of harmonic oscillation. presented for a different processing methods. Dashed lines separate central sector (the sample) and side sectors (the background)

Then, the differences are computed by the following equation (1):

$$D = |mean(S) - mean(B)| \tag{1}$$

where: *D*-horizontal or vertical difference value for the chosen method, *S*-values of the sample sector, *B*-values of the background sector.

A value of the *D* parameter for all considered variations is presented in Tab. 4.

Tab. 4. Difference between mean of background and sample surface (example sectors in figure above). Chosen methods are underlined and bolded

	Method	Horizontal	Vertical	Processing Time, s
Lock-in 0.016 Hz	PCT	0.0927	0.1344	48.58
	FFT Ampl.	0.1102	0.1577	16.41
	FFT Phase	**<u>0.3511</u>**	**<u>0.2202</u>**	**<u>16.41</u>**
	CorrelContr	0.1485	0.1885	12.27
	Histogram	0.7246	0.0227	7.2
Pulse Thermo-graphy 550,	PCT	0.0408	0.0808	35.73
	FFT Ampl.	0.4529	0.1739	7.56
	FFT Phase	0.1117	0.0684	7.56
	CorrelContr	**<u>0.4064</u>**	**<u>0.3072</u>**	**<u>10.85</u>**
	Histogram	0.7923	0.165	6,31
Pulse Thermograp hy 750 ms	PCT	0.0546	0.0956	37.9
	FFT Ampl.	0.4622	0.1646	11.65
	FFT Phase	0.1302	0.0897	11.65
	CorrelContr	**<u>0.3999</u>**	**<u>0.3146</u>**	**<u>13.97</u>**
	Histogram	0.79	0.1156	6.32

It is possible to proof the previous considerations. Vertical sample-background ratio *D* is the best for FFT Phase value and Correlated Contrast in respect to the LT and PT methods accordingly. Moreover, in the chosen methods, the horizontal values are even higher than vertical ones. The time of processing is also acceptable for all situations. Although, there are methods, where horizontal values are higher than in the chosen ones (Histogram, FFT Amplitude in some cases), but the vertical value of *D* parameter isn't at acceptable level.

4. ROI extraction algorithm

Thresholding is a natural, another step to extract ROI field of the observed samples. It is highly required because the images still preserve local regions of noise and discontinuities. There are several methods, which allow to clear sectors from the artifacts.

For this case the Fixing Holes (Matlab build-in function) and erosion method were chosen. The final step is to draw a rectangular sector which coordinates allows to separate appropriate ROI part from the image. An, overall algorithm, which contains mentioned steps is presented in Fig. 4.

The algorithm has been implemented and executed for every IR sequence from the data base. Last step of ROI selection procedure executed for DIS5 sample Phase Image as an example is visible in Fig. 5.

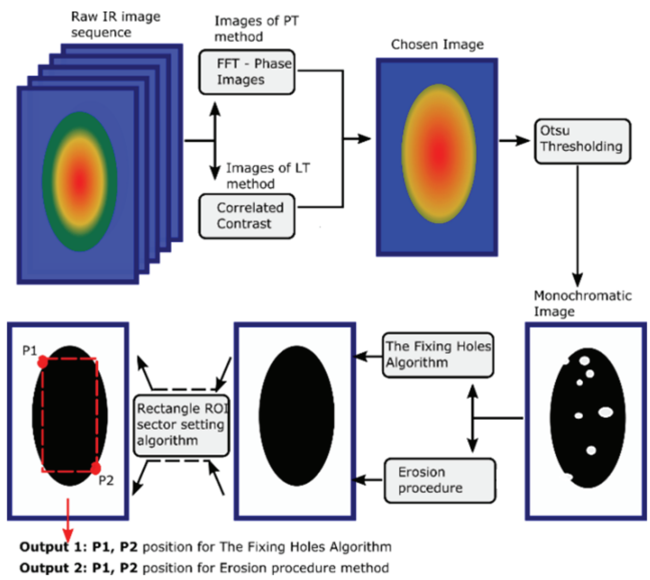

Fig. 4. Diagram of ROI extraction algorithm

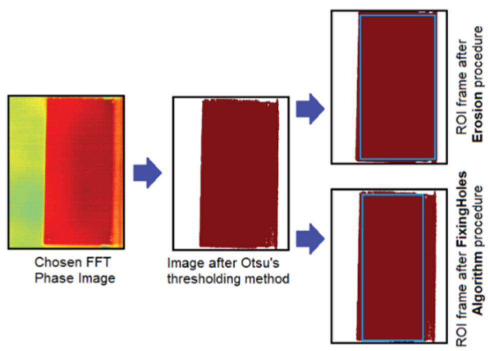

Fig. 5. Example of result images made during the ROI extraction procedure, executed for Hole Fixing and erosion. Chosen FFT Phase image were generated form IR image sequence of front side *DIS5* sample

5. Results

To assess efficiency of the results, manual ROI sectors were set for every case, as a base to measure error value. Error has been described according to the equation Eq.2:

$$b = \frac{|x_1 - \hat{x}_1| + |x_2 - \hat{x}_2| + |y_1 - \hat{y}_1| + |y_2 - \hat{y}_2|}{|\hat{x}_2 - \hat{x}_1| + |\hat{y}_2 - \hat{y}_1|} \cdot 100\%, \quad (2)$$

where: $\hat{x}_1, \hat{x}_2$ - bottom and top vertical position of manual ROI rectangle, $\hat{y}_1, \hat{y}_2$ - left and right horizontal position of manual ROI rectangle, $x_1, x_2, y_1, y_2 -$ same as above according to ROI of Erosion or HoleFixing method (Fig. 6).

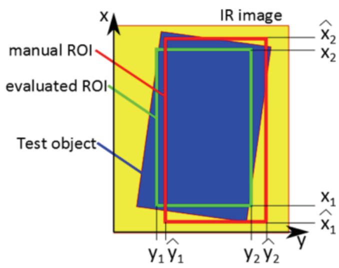

Fig. 6. Visual idea of error estimation

Overall error value of every sample, method and ROI extraction method type is summarized in Tab. 5.

It is more than visible that presented results are divergent. The error changes between 0.61% and 18.77%, but in general, Matlab's Hole Fixing function has a smaller mean error in every case. Although, overall differences between a manual and the algorithm ROI are relatively small (about 6%). The main reason of the divergence could be caused by an angular misalignment, which was omitted in the ROI extraction procedure.

Tab. 5. Error table

Sample description		Erosion			HoleFixing		
		LT 0.016 Hz	PT 550 ms	PT 750 ms	LT 0.016 Hz	PT 550 ms	PT 750 ms
GR	Front	2.30%	6.66%	8.96%	2.06%	4,72%	5.57%
	Back	3.27%	5.08%	4.84%	4.72%	1.94%	1.69%
DIS5	Front	5.69%	4.48%	7.02%	4.24%	1.82%	3.63%
	Back	1.21%	6.54%	4.24%	2.66%	3.15%	2.30%
DIS10	Front	3.15%	12.47%	13.80%	1.69%	9.08%	10.65%
	Back	1.57%	6.78%	11.50%	2.06%	3.39%	8.11%
DIS15	Front	5.69%	5.45%	5.57%	4.24%	2.54%	2.18%
	Back	2.54%	13.44%	16.46%	1.09%	11.02%	13.08%
OIL1	Front	3.51%	5.57%	12.83%	2.06%	3.15%	9.44%
	Back	2.54%	6.78%	6.42%	2.06%	3.39%	3.03%
OIL2	Front	2.54%	6.42%	6.17%	0.85%	3.03%	2.78%
	Back	3.15%	5.33%	6.66%	2.42%	2.18%	3.27%
WV	Front	2.66%	6.30%	5.21%	2.18%	2.91%	1.82%
	Back	2.54%	5.69%	5.93%	1.57%	2.30%	2.54%
SZC	Front	4.00%	9.08%	7.38%	0.61%	5.69%	4.48%
	Back	3.51%	6.05%	4.84%	2.06%	2.91%	1.45%
POG	Front	2.78%	10.65%	18.77%	3.03%	7.99%	15.38%
	Back	4.00%	13.08%	13.68%	3.27%	9.93%	10.53%
VAR	Front	3.63%	8.35%	7.38%	2.66%	4.96%	4.24%
	Back	4.84%	5.81%	9.56%	2.91%	2.42%	6.17%
TRI	Front	1.69%	5.21%	7.63%	1.69%	2.06%	4.24%
	Back	4.24%	8.11%	8.11%	3.03%	4.72%	4.96%
Mean		**3.23%**	**7.42%**	**8.77%**	**2.42%**	**4.33%**	**5.52%**

6. Conclusions

Solution presented in this paper allows to automatically extract sample surface from IR image and set ROI coordinates. Two stages algorithm was presented. The key point was to find good method for filling discontinuities in sample region after segmentation. The Fixing Holes algorithm gave best results. Analysis of obtained results lead to a conclusion, that segmentation accuracy depends on many reasons, and varies significantly. Most possible reasons are connected with arbitrary chosen processing methods and angular misalignment of the samples. A small precision of manually set sample coordinates could be an additional problem. Further studies should be focused on implementation of advanced processing methods and use of angular information of the sample to reduce foreground object extraction error. Additionally studies on elimination of other distortions by image rectification should be performed.

7. References

[1] Rajeshwar Dass, Priyanka, Swapna Devi: Image Segmentation Techniques. International Journal of Electronics & Communication Technology. Vol. 3, 2012, p. 66-70.

[2] Larsen Cory A.: Document Flash Thermography. A thesis submitted in partial fulfillment of the requirements for the degree of MASTER OF SCIENCE in Electrical Engineering, Utah State University 2011, https://pdfs.semanticscholar.org/c4e5/66f8c8e6177a242fd55f1794db8 2ffba21ee.pdf

[3] Maldague X.: Theory and practice of infrared technology for nondestructive testing. Michigan University, Wiley, 2001.

[4] FLIR Systems introduces Multi Spectral Dynamic Imaging (MSX), Press Release of FLIR Commercial Systems B.V., http://www.flir.co.uk/cs/display/?id=56012

[5] Ratna Sulistiyanti S., Arinto Setyawan F.X., Susanto Adhi: Histogram Characterizations of Infrared Images Captured by a Modified Digital Camera. International Journal of Electronic Engineering Research ISSN 0975 - 6450 Volume 1 Number 4 (2009) pp. 329–336.

[6] Gonzalez R. C. and Woods R. E.: Digital Image Processing. Upper Saddle River: Pearson Education, Inc., 2008.

[7] Klein M. T., Ibarra-Castanedo C., Bendada A. & Maldague X. P.: Thermographic signal processing through correlation operators in pulsed thermography. 2008, March. In Proc. of SPIE Vol (Vol. 6939, pp. 693915-1).

[8] Ibarra-Castanedo C., Avdelidis N. P., Grenier M., Maldague X., Bendada A.: Active thermography signal processing techniques for defect detection and characterization on composite materials. 2010, Proc. of SPIE Vol. 7661 76610O-2.

Received: 01.11.2016 Paper reviewed Accepted: 03.03.2017

Michał KURPIŃSKI, MSc

Michał Kurpiński is an graduate at the Faculty of Mechanical Engineering of Silesian University of Technology. He received MSc degree in 2013. Currently, He is on PhD studies in the Institute of Fundamentals of Machinery Design at the Faculty of Mechanical Engineering of the Silesian University of Technology since 2013. At present, he is doing research related with usage of NDE active thermography methods for industrial application.

e-mail: michal.kurpinski@polsl.pl

Wojciech JAMROZIK, PhD, eng.

Since 2012 he is employed at Silesian University of Technology, Institute of Fundamentals of Machinery Design. His scientific interests are connected with technical diagnostics, thermovision, image processing and analysis, as well as reasoning methods under uncertainty.

e-mail: wojcich.jamrozik@polsl.pl